

Sergey FILIPKOVSKIY, Evgen POLYAKOV

National Aerospace University "Kharkiv Aviation Institute", Ukraine

## DEVELOPMENT AND MODAL ANALYSIS OF A DISCRETE MODEL OF A WING WITH ENGINE

*The object of this study is the vibrations of a wing with an engine. This study aims to develop a model with the smallest possible number of degrees of freedom (DOF) for solving the influence of imbalance and engine axis tilt on aeroelastic oscillations of the wing console.*

*Current economic constraints and environmental regulations require the development of more efficient aircraft configurations. The observed trend in aircraft design to reduce aerodynamic drag and fuel consumption and emissions is to increase the wing aspect ratio. However, under the same operating conditions, a thin wing is more flexible and subject to higher deflections. This effect can lead to changes in the dynamic behavior and aeroelastic response, potentially leading to instability. Following the requirements of AC 25.629-1B, the absence of aeroelastic instability must be demonstrated for all speed and altitude combinations. In this case, all possible engine operating conditions and combinations of conditions must be considered to consider the influence of gyroscopic loads and thrust on aeroelastic stability.*

*A review of publications showed that models with a maximum of three DOF are used to study the aeroelasticity of a high aspect ratio powered wing.*

*A discrete wing model with an engine has been developed. This model has 23 DOF. This model significantly expands the capabilities of the numerical analysis of aeroelastic oscillations compared with the generally accepted model with three DOF, which reduces wing oscillations to oscillations of an average profile. This number of DOF is sufficient to approximate the shapes of the wing's bending and torsional oscillations in the frequency range up to the engine speed. A rotating imbalance force can be applied to the concentrated mass, which models the engine at the pylon end. The effect of imbalance in any given plane on the dynamics of the model can be investigated to meet the requirements of AC 25.629-1B. Modal analysis of the discrete model was performed. The obtained frequencies and modes of oscillations were similar to those of the high aspect ratio wing of a transport aircraft. In the future, this model will be used to investigate the effect of engine imbalance and tilt on aeroelastic oscillations, flutter, and the transition to limit wing oscillation cycles.*

**Keywords:** wing; engine; vortex flutter; model; degrees of freedom; modal analysis.

### Introduction

Current economic constraints and environmental regulations require the development of more efficient aircraft configurations. The observed trend in aircraft design to reduce aerodynamic drag, as well as to reduce fuel consumption and emissions, is to increase the wing aspect ratio. However, a thin wing is more flexible and subject to higher deflections under the same operating conditions. This effect can lead to changes in dynamic behavior and aeroelastic response, potentially leading to instability. It is therefore important to consider geometric nonlinearities when designing high aspect ratio wings, and to have accurate calculation programs that link aerodynamic and structural models in the presence of nonlinearities.

In accordance with the requirements of AC 25.629-1B, the absence of aeroelastic instability must be demonstrated for all combinations of speed and altitude. In this case, all possible engine operating conditions and

combinations of conditions must be considered, from idle power to maximum available thrust, including cases of one engine stopped and windmilling, in order to take into account the influence of gyroscopic loads and thrust on aeroelastic stability [1].

The aeroelastic stability assessment shall include investigations of any significant elastic, inertial and aerodynamic forces, including those associated with rotation and in-plane translation of any turbopropeller or propeller, including propeller or fan blade aerodynamics, powerplant elasticity, powerplant mounting characteristics, and gyroscopic coupling; the effects of engine mount, engine gearbox mount or shaft failures that result in propeller hub axis shift during pitch or yaw movements [1].

The structural aspect of aeroelastic modeling typically involves approximating the aircraft wing in its simplest structural form as a long, thin, and symmetrical plate with uniformly distributed mass and structural properties. Due to the uniformity and symmetry of such



a plate, a complete understanding of its dynamic behavior can be obtained by observing only one cross-section, known as the typical wing section [2, 3]. With such structural approximations, this reduces the three-dimensional aeroelastic problem to a two-dimensional problem.

Another important model is the pseudo-model of two degrees of freedom (DOF) with bending and pitching. Similar to the cantilever plate, there are two-dimensional flexible airfoils that are modeled as finite beam elements with chord bending, capable of bending and twisting [4].

The interaction of the pitch and bending DOF with the additional offset from the attached element leads to multiple flutter phenomena that cannot be observed in two DOF models. More realistic aeroelastic modeling requires consideration of three or more DOF.

The action of rotating parts of a turboprop power plant (propeller and gas turbine engine rotor) causes whirl flutter. The physical principles of whirl flutter are explained using a simple mechanical system with two DOF. In the book [5], an analytical solution is given to determine the aerodynamic forces caused by gyroscopic motion on each of the propeller blades and the influence of the main structural parameters on the whirl flutter stability are discussed.

In article [6], an aeroelastic method developed for the study of propeller flutter is presented and tested. Propeller flutter can take various forms, with stall, whirl, and classical flutter being the primary responses. In [7], the effects of blade elasticity, wing/pylon model, density, speed of sound, unstable aerodynamics, and realistic airfoil tables on whirl flutter velocity are considered. The paper [8] investigates the influence of a freeplay structural nonlinearity on the degree of freedom of the nacelle pitch. Two rotor-nacelle models of contrasting complexity are studied: one represents the classic whirl flutter (propellers), and the other captures the main effects of tiltrotor aeroelasticity (proprotors).

Most of the whirl flutter stability analyses in the current literature are based on linear theory, which does not fully capture the effects of nonlinearity [9]. Instead, continuation and bifurcation methods (CBM) can be used to fully evaluate and analyze the effects of the presence of nonlinearity. A 9-DOF model with quasi-stable aerodynamics, a flexible wing and blades that can move both cyclically and jointly in both flapping and lead-lag motions, producing a gimbal flap-like behavior, was adopted from the existing literature. [10] presents methodologies used to analyze the stability of systems subjected to periodic aerodynamic excitation when the problem is modeled using full-featured multibody solvers, in support of whirl flutter identification during wind tunnel testing. In [11], frequency domain transfer matrices for propeller hub loads determined using a time-

dependent multibody simulation model of an isolated turboprop propeller are included in a frequency domain flutter analysis to study the effect of blade elasticity on propeller whirl flutter.

A study [12] shows how the critical speed of wing-propeller systems depends on the mounting stiffness and the propeller position. Weak mounting stiffness leads to whirl flutter, while rigid mounting stiffness leads to wing flutter. In the latter case, the propeller position along the wing span can change the wing mode shapes and hence the flutter mechanism.

A review of publications showed that models with a maximum of three DOF are used to study flutter. Such a model replaces the wing with its section, in which the DOF are the vertical movement of the profile, its pitch rotation, plus either an aileron rotation or a suspended magazine deflection. In a powered wing, as a rule, the engine is located closer to the wing root, and the greatest elastic deformations are observed at the end of the console. Therefore, more than three DOF are required to study the aeroelasticity of a high aspect ratio powered wing.

The object of study is the vibrations of a wing with an engine. The purpose of this article is to develop a model with the smallest possible number of DOF for solving problems of the influence of imbalance and engine axis tilt on aeroelastic oscillations of the wing console.

## 1. Beam Model

The simplest model with a finite number of DOF for studying the vibrations of a high aspect ratio wing with an engine is a beam consisting of several elements [15]. The rigidity of each element is equal to the rigidity of the corresponding section of the wing, and the masses with moments of inertia are concentrated in the sections in which the elements are connected. The DOF are the deflections and rotation angles of the beam sections in which the elements are connected. In the wing, the centers of mass of the sections are shifted relative to the elastic axis (Fig. 1). Therefore, instead of one mass, we place a pair of concentrated masses in the sections. We fix one of the masses on a rigid arm relative to the elastic axis to ensure a given position of the center of mass and the moment of inertia (Fig. 2).

The wing shown in Fig. 1 has a half-span of  $L = 16.0$  m, a root chord of  $b_r = 4.85$  m, a tip chord of  $b_t = 1/45$  m, and the position of the elastic axis relative to the leading edge of  $X_0/b = 0.37$ . Table 1 gives the stiffness and inertial parameters in five sections of the wing, where  $Z$  is the distance from the root,  $m$  is the linear mass,  $\sigma_x$  is the position of the center of mass relative to the elastic axis ( $\sigma_x > 0$  means the center of mass is behind the elastic axis),  $I_{mz}$  is the linear moment of inertia of the section,  $GJ_k$  is the torsional rigidity,  $EI_z$  is the bending rigidity in the vertical plane,  $EI_y$  is the

bending rigidity in the horizontal plane. The directions of the axes are shown in Fig. 2.

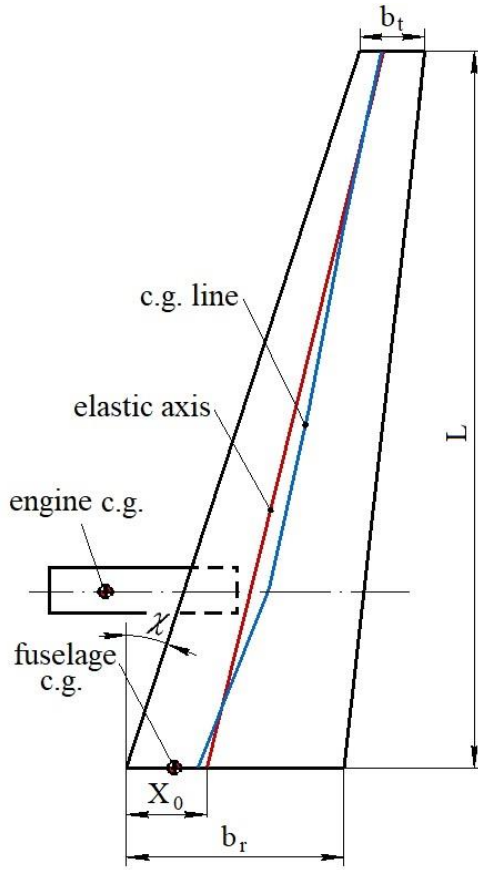


Fig. 1. Masses and elastic axis of the wing

The engine is approximated by a concentrated mass at the end of the pylon, the mass of the engine with the nacelle  $M_e = 2917$  kg, the moments of inertia  $I_{ex} = 1525$  kg·m<sup>2</sup>,  $I_{ey} = 4420$  kg·m<sup>2</sup>,  $I_{ez} = 4582$  kg·m<sup>2</sup>. The engine is lowered relative to the wing plane by 0.6 m. The length of the pylon  $X_p = 2.39$  m, the rigidity parameters are as follows:  $EI_{zp} = 2.9 \cdot 10^7$  N·m<sup>2</sup>,  $EI_{yp} = 0.6 \cdot 10^7$  N·m<sup>2</sup>,  $GJ_{kp} = 0.4 \cdot 10^7$  N·m<sup>2</sup>.

The fuselage with the tail unit is approximated by a concentrated mass, which is attached to the root chord of the wing. The mass of the fuselage with the tail unit is  $M_f = 13403$  kg, the moments of inertia are  $I_{fx} = 6.1 \cdot 10^4$  kg·m<sup>2</sup>,  $I_{fy} = 5.7 \cdot 10^5$  kg·m<sup>2</sup>,  $I_{fz} = 6.0 \cdot 10^5$  kg·m<sup>2</sup>.

## 2. Finite Element Model

We construct the finite element model in the ANSYS software package. We use beam finite elements BEAM188 with two nodes and six DOF in the node. We use elements whose cross-section changes linearly along the length. We use a box section (Fig. 3) so that the rigidity properties of the beam match the properties of the wing. The moments of inertia, on which the rigid-

ity parameters of such a cross-section depend, can be written using the following formulas [16]:

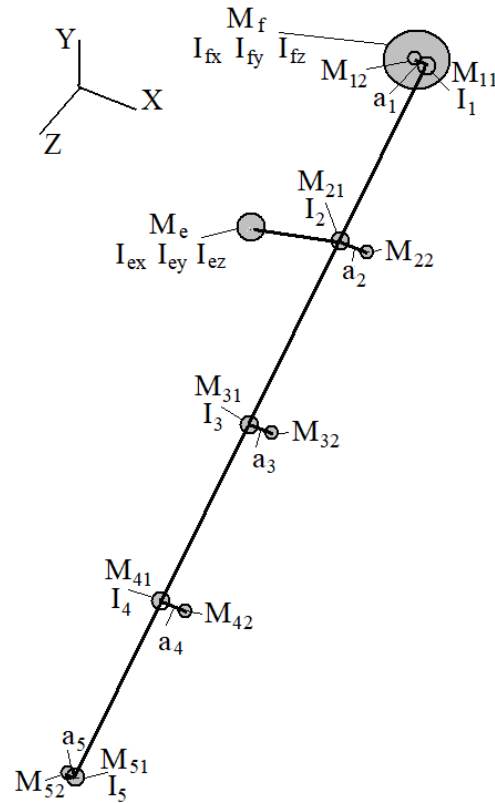


Fig. 2. Beam model of the wing

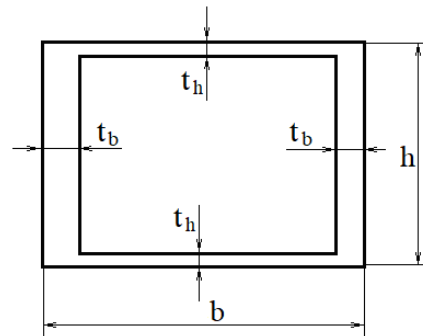


Fig. 3. Cross-section of the beam

$$J_k = \frac{2(h - t_h)^2(b - t_b)t_h t_b}{(h - t_h)t_h + (b - t_b)t_b}, \quad (1)$$

$$I_z = \frac{bh^3 - (b - 2t_b)(h - 2t_h)^3}{12}, \quad (2)$$

$$I_y = \frac{b^3h - (b - 2t_b)^3(h - 2t_h)}{12}. \quad (3)$$

We select an aluminum alloy as the beam material, which has an elastic modulus  $E = 7.1 \cdot 10^{10}$  Pa, Poisson's ratio  $\mu = 0.32$ , density  $\rho = 2700$  kg/m<sup>3</sup>, shear modulus

$G = E / 2(1+\mu) = 2.7 \cdot 10^{10}$  Pa. Thus, we have obtained a system of three equations with four unknowns for each of the five sections. To select the dimensions of the sections, we set one of the dimensions, the rest are obtained by solving the system of equations (1) – (3).

We determine the linear masses of the obtained sections using the formula

$$\rho F = \rho [bh - (b - 2t_b)(h - 2t_h)], \quad (4)$$

where  $F$  is the cross-section area. The linear masses  $\rho F$  obtained less than the specified linear masses in Table 1. To obtain such inertial characteristics of the beam sections as specified in Table 1, we add a concentrated mass  $M_{i1}$  with a moment of inertia  $I_i$  in each section, where  $i$  is the section number. To shift the center of mass of the section relative to the elastic axis, as specified in Table 1, we add a balancing mass  $M_{i2}$  on a rigid bracket of size  $a_i$  (Fig. 2). We use finite elements MASS21 as masses. We use the same beam elements with high rigidity and zero density as brackets.

Let us write down the equations for determining the additional masses and moments of inertia (we omit the section number).

$$m = \rho F + \frac{M_1 + M_2}{l}, \quad (5)$$

$$\sigma_x = \frac{M_2 a}{\rho F l + M_1 + M_2}, \quad (6)$$

$$I_{mz} = \rho(I_z + I_z) + \frac{I_1 + M_2 a^2}{l}, \quad (7)$$

where  $l$  is the length of the part of the beam that is adjacent to the mass  $M_1$ , for the extreme nodes  $l = L / 8$ , for the remaining nodes  $l = L / 4$ . We have obtained a system of three equations with four unknowns for each of the five sections. To obtain a solution, we set the size  $a$ , the masses and the moment of inertia are obtained by

solving the system of equations (5) – (7). Table 2 contains the results of the calculations of the beam sections.

The pylon is modeled by a single box-section beam element. The section dimensions  $b = 0/8247$  m,  $h = 0/2890$  m,  $t_b = 0.0009$  m,  $t_h = 0.0056$  m are calculated using formulas (1) – (3). The engine and fuselage with tail unit are modeled using MASS21 finite elements.

### 3. Modal analysis of the finite element model

Modal analysis is performed to determine the frequencies and modes of free vibrations. As a rule, the lowest frequencies and modes of free vibrations are determined during aircraft bench tests. By comparing the calculated and experimental results of modal analysis, it is possible to check how accurately the finite element model approximates the wing. The results of modal analysis are then used to analyze forced vibrations and motion stability.

The constructed model has 11 nodes and, accordingly, 66 DOF. The aircraft wing can bend in the vertical plane and twist around the rigidity axis during oscillations. Therefore, we can leave only those DOF that allow these movements, and fix the rest. For all wing console nodes, we fix the DOF in the XZ plane (movements along the X, Z axes and rotation around the Y axis). The balancing masses on rigid brackets do not have moments of inertia, so we can also fix their rotations around the X and Z axes. We will study only symmetrical oscillation modes, so we fix the root section rotation along the roll (around the X axis) and allow only the pitch rotation. For the engine at the end of the pylon, we fix the movement along the longitudinal X axis and the rotation around this axis. The model with 23 DOF remains.

Table 1

Inertial parameters of wing sections

Z/L	m, kg/m	$\sigma_x$ , m	$I_{mz}$ , kg·m	$GJ_k$ , N·m <sup>2</sup>	$EI_z$ , N·m <sup>2</sup>	$EI_y$ , N·m <sup>2</sup>
0.00	200	-0.20	200	$8.0 \cdot 10^7$	$15.0 \cdot 10^7$	$60.0 \cdot 10^7$
0.25	190	0.40	250	$5.0 \cdot 10^7$	$10.0 \cdot 10^7$	$40.0 \cdot 10^7$
0.50	120	0.30	100	$1.3 \cdot 10^7$	$3.0 \cdot 10^7$	$10.0 \cdot 10^7$
0.75	70	0.08	20	$0.25 \cdot 10^7$	$0.65 \cdot 10^7$	$3.0 \cdot 10^7$
1.00	21	-0.05	3	$0.1 \cdot 10^7$	$0.15 \cdot 10^7$	$1.0 \cdot 10^7$

Table 2

Parameters of the wing beam model sections

Z/L	b, m	h, m	$t_b$ , m	$t_h$ , m	a, m	$I_1$ , kg·m <sup>2</sup>	$M_1$ , kg	$M_2$ , kg
0.00	1.6026	1.1248	0.0055	0.0008	-0.3	318.95	52.575	266.66
0.25	2.1391	1.5310	0.0015	0.0002	0.5	771.94	92.579	608.00
0.50	1.0485	0.8451	0.0029	0.00035	0.4	322.62	59.081	360.00
0.75	0.6913	0.4851	0.0035	0.0003	0.4	65.487	182.44	56.000
1.00	0.5343	0.2730	0.0033	0.0005	-0.1	4.9153	8.2992	21.000

The model is not fixed along the Y axis, so the lower frequency is zero and this frequency corresponds to the model's movement as a rigid body in the direction

of this axis. The remaining frequencies correspond to elastic oscillations of the model (Fig. 4).

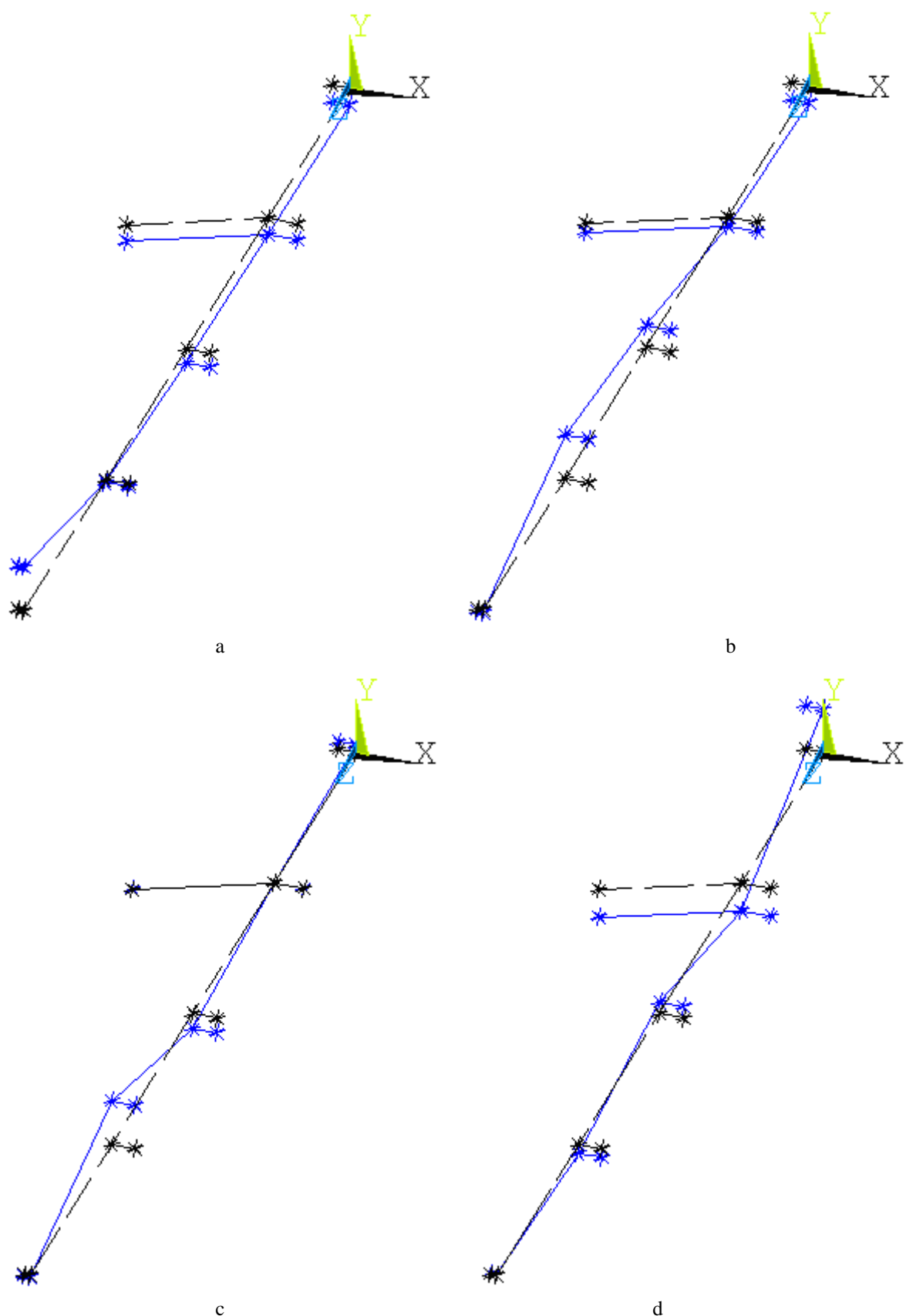
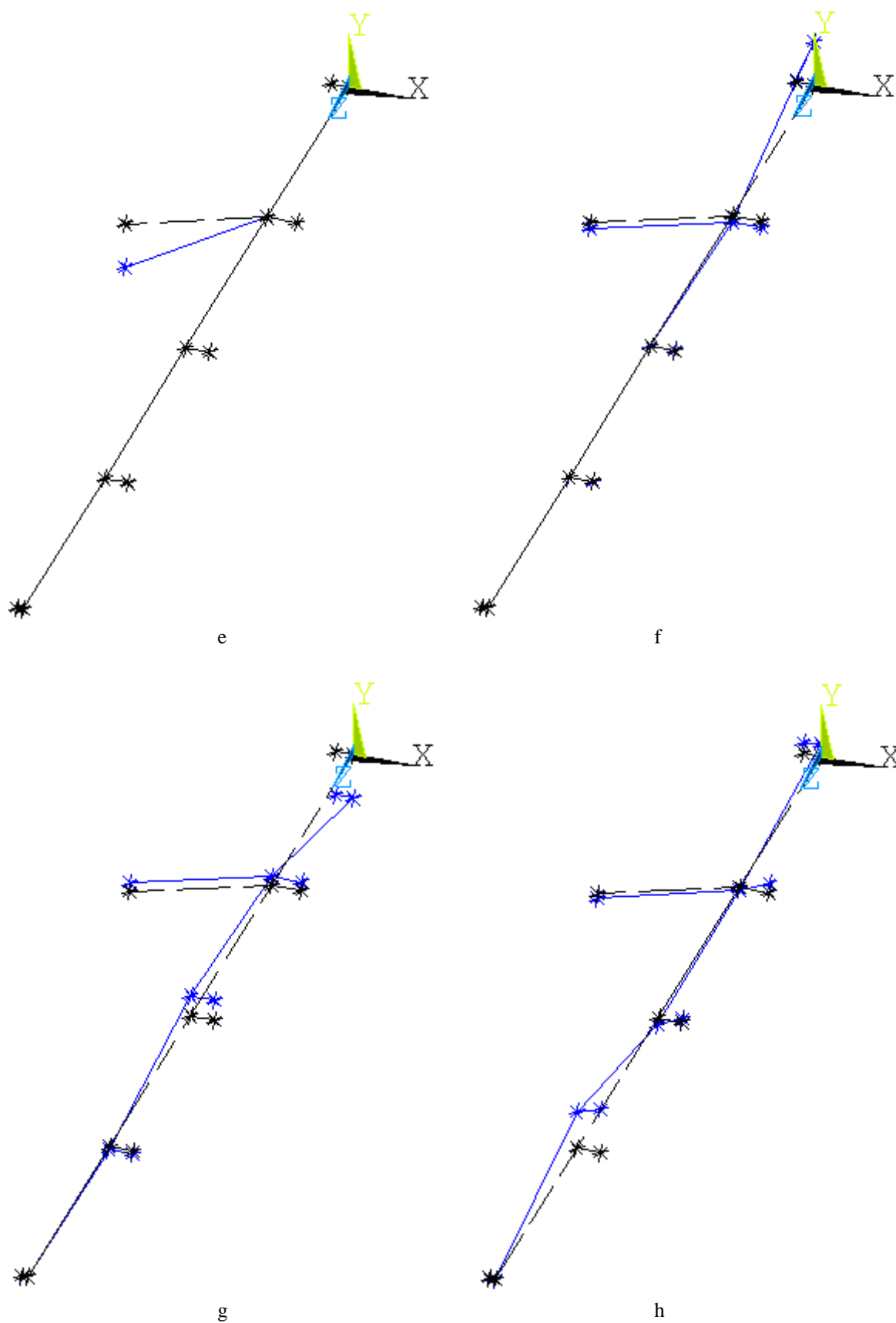


Fig. 4. Natural vibration modes of a discrete model



Continuation of the Fig. 4. Natural vibration modes of a discrete model

The first mode of oscillation (Fig. 4,a) is bending with one node near the section  $Z = 0.75 L$ , it has a frequency of 5.24 Hz. The greatest deflection of the wing model occurs at the end of the console.

The second, third and fourth modes of vibration (Fig. 4,b, c, d) are also bending, with two, three and four nodes respectively and have frequencies of 21.80, 32.55 and 43.31 Hz. The last node of these three modes is located near the end section, and the remaining nodes are distributed evenly along the length of the console. The greatest deflection of the second and third modes is observed in the section  $Z = 0.75 L$ , and the fourth mode in the section  $Z = 0.25 L$ . The fifth mode of oscillation (Fig. 4,e) has a frequency of 75.25 Hz and represents oscillations of the engine on the pylon. In the figure, the pylon is shown as a straight line in a deformed state because in the ANSYS graphic window, the nodes are connected by straight lines; in reality, the pylon axis is curved. The wing console is practically not deformed.

The sixth, seventh and eighth modes of oscillation are bending-torsional, they have frequencies of 79.06, 103.96 and 126.47 Hz respectively. The sixth mode shows rotation and deflection of the root section relative to the wing console axis (Fig. 4,f). The seventh mode shows more deflections than torsion. The eighth mode (Fig. 4,g) shows rotations of the root section and the  $Z = 0.25 L$  section in opposite directions together with deflections along the entire length of the console. The eighth mode of elastic oscillations (Fig. 4,h) has a frequency that slightly exceeds the rotation frequency of the fan rotor.

## Conclusions

A discrete model of a wing with an engine has been developed. This model has 23 DOF. This model significantly expands the capabilities of the numerical analysis of aeroelastic oscillations compared to the generally accepted model with three DOF, which reduces wing oscillations to oscillations of an average profile. This number of DOF is sufficient to approximate the shapes of bending and torsional oscillations of the wing in the frequency range up to the engine speed. A rotating imbalance force can be applied to the concentrated mass, which models the engine at the end of the pylon. The effect of imbalance in any given plane on the dynamics of the model can be investigated in order to meet the requirements of AC 25.629-1B [1]. In the future, this model will be used to investigate the effect of engine imbalance and tilt on aeroelastic oscillations, flutter, and the transition to limit cycles of wing oscillations.

A modal analysis of the discrete model was performed. The frequencies and modes of oscillations ob-

tained were similar to those of the high aspect ratio wing of a transport aircraft.

**Contributions of authors:** formulation of tasks – **Sergey Filipkovsky**, development of model, analysis of results, visualization – **Sergey Filipkovsky**, **Evgen Polyakov**; writing – review and editing – **Sergey Filipkovsky**.

## Conflict of interest

The authors declare that they have no conflict of interest in relation to this research, whether financial, personal, authorship or otherwise, that could affect the research and its results presented in this paper.

## Financing

The study was conducted without financial support.

## Data availability

The Manuscript has no associated data.

## Use of Artificial Intelligence

The authors confirm that they did not use artificial intelligence methods while creating the presented work.

All the authors have read and agreed to the published version of this manuscript.

## References

1. *Advisory Circular No 25.629-1B. U.S. Department of Transportation*. Federal Aviation Administration, 2014. 22 p Available at: [https://www.faa.gov/documentLibrary/media/Advisory\\_Circular/AC\\_25\\_629-1B.pdf](https://www.faa.gov/documentLibrary/media/Advisory_Circular/AC_25_629-1B.pdf)
2. Dowell, E. H. A modern course in aeroelasticity, Solid mechanics and its applications. 6<sup>th</sup> edn, Springer International Publishing Switzerland, 2015. 828 p.
3. Hodges, D. H., Pierce, G. A. Introduction to structural dynamics and aeroelasticity. 2<sup>nd</sup> edn, Cambridge University Press, 2011. 271 p. doi: 10.1017/CBO9780511997112
4. Hefeng, D. Chenxi, W. Shaobin, L. Zhen, S. Numerical research on segmented flexible airfoils considering fluid-structure interaction. *Procedia Engineering*. 2015, vol. 99, pp. 57–66, doi: 10.1016/j.proeng.2014.12.508.
5. Čečrdle, J. Whirl flutter of turboprop aircraft structures. 2<sup>nd</sup> edn, Woodhead Publishing, 2015. 344 p.
6. Higgins, R. J. Jimenez-Garcia, A. Barakos, G. N., & Bown, N. High-fidelity computational fluid dynamics methods for the simulation of propeller stall flutter. *AIAA Journal*. 2019, vol. 57, no 12, pp. 5281–5292. doi: 10.2514/1.J058463.
7. Yeo, H., & Kreshock, A. R. Whirl flutter investigation of hingeless propellers. *Journal of Aircraft*. 2020, vol. 57, no. 4, pp. 558–568. doi: 10.2514/1.C035609.

8. Mair, C., Titurus, B., & Rezgui, D. Stability analysis of whirl flutter in rotor-nacelle systems with freeplay nonlinearity. *Nonlinear Dynamics*. 2021, vol. 104, pp. 65–89. doi: 10.1007/s11071-021-06271-z.
9. Mair, C., Rezgui, D., & Titurus, B. Stability and dynamical analysis of whirl flutter in a gimbaled rotor-nacelle system with a smooth nonlinearity. *The Aeronautical Journal*. 2023, vol. 127, pp. 1234–1254. doi: 10.1017/aer.2023.10.
10. Cocco, A. Mazzetti, S. Masarati, P. Hoff, S. & Timmerman, B. Numerical whirl-flutter analysis of a tiltrotor semi-span wind tunnel model. *CEAS Aeronautical Journal*. 2022, vol. 13, pp. 923–938. doi: 10.1007/s13272-022-00605-2.
11. Koch, C., & Koert, B. Including blade elasticity into frequency-domain propeller whirl flutter analysis. *Journal of Aircraft*, 2024, vol. 61, no 3, pp. 774–784. doi: 10.2514/1.C037501.
12. Böhnisch, N. Braun, C. Muscarello, V. & Marzocca, P. About the wing and whirl flutter of a slender wing-propeller system. *Journal of Aircraft*, 2024, vol. 61, no. 4, pp. 1117–1130. doi: 10.2514/1.C037542.
13. Bisplinghoff, R. L., Ashley, H., & Halfman, R. L. *Aeroelasticity*. Courier Corporation, NY, 2013. 880 p.
14. Timoshenko, S. Strength of materials. Part 2. Advanced theory and problems. 2<sup>nd</sup> edn. D. Van Nostrand Company, NY, 1947. 524 p.

Поступила до редакції 05.05.2025, розглянута на редколегії 18.08.2025

## РОЗРОБКА ТА МОДАЛЬНИЙ АНАЛІЗ ДИСКРЕТНОЇ МОДЕЛІ КРИЛА З ДВИГУНОМ

С. В. Філіповський, Є. Ю. Поляков

Об'єктом дослідження є коливання крила з двигуном. Мета роботи – розробити модель з якомога меншою кількістю ступенів свободи для вирішення завдань впливу дисбалансу та перекосу осі двигуна на аеропружні коливання консолі крила.

Поточні економічні обмеження та екологічні норми вимагають розробки найефективніших змін літаків. Спостережувана тенденція до зниження опору конструкції літаків, викликаного аеродинамічною силою, а також зниження витрати палива й викидів шкідливих речовин пов'язана зі збільшенням подовження крила. Однак тонке крило є гнучкішим і схильне до більших відхилень у тих же умовах експлуатації. Цей ефект може призвести до змін динамічної поведінки та аеропружної реакції, що потенційно може призвести до нестабільності. Відповідно до вимог АС 25.629-1В, відсутність аеропружної нестійкості має бути показана для всіх комбінацій швидкості та висоти польоту. При цьому треба розглянути всі можливі режими роботи двигуна та комбінації режимів з метою врахування впливу гіроскопічних навантажень і тяги на аеропружну стійкість.

Огляд публікацій показав, що при дослідженні флатера використовуються моделі, які мають максимум три ступеня свободи, щоб досліджувати аеропружність крила великого подовження з двигуном. Розроблено дискретну модель крила з двигуном, яка має 23 ступеня свободи. Така модель суттєво розширює можливості чисельного аналізу аеропружних коливань порівняно із загальноприйнятою моделлю з трьома ступенями свободи, яка зводить коливання крила до коливань усередненого профілю. Такої кількості ступенів свободи достатньо для того, щоб апроксимувати форми згинальних і крутильних коливань крила на діапазоні частот аж до частоти обертання двигуна. До зосередженої маси, яка моделює двигун на кінці пілона, можна прикласти обертову силу дисбалансу. Можна дослідити вплив дисбалансу в будь-якій заданій площині на динаміку моделі, щоб задовольнити вимоги АС 25.629-1В.

Виконано модальний аналіз дискретної моделі. Отримані частоти та форми коливань аналогічні частотам і формам коливань крила великого подовження транспортного літака. Надалі за допомогою цієї моделі можна буде дослідити вплив дисбалансу та перекосу двигуна на аеропружні коливання, флатер і перехід до граничних циклів коливань крила.

**Ключові слова:** крило; двигун; вихровий флаттер; модель; ступінь свободи; модальний аналіз.

**Філіповський Сергій Володимирович** – д-р техн. наук, проф., проф. каф. проектування літаків і вертольотів, Національний аерокосмічний університет «Харківський авіаційний інститут», Харків, Україна.

**Поляков Євген Юрійович** – асп. каф. проектування літаків і вертольотів, Національний аерокосмічний університет «Харківський авіаційний інститут», Харків, Україна.

**Sergey Filipkovskij** – Doctor of Science (Engineering), Professor, Professor at the Department of Airplanes and Helicopters Design, National Aerospace University "Kharkiv Aviation Institute", Kharkiv, Ukraine, e-mail: s.filipkovskij@khai.edu, ORCID: 0000-0003-2861-8032, Scopus Author ID: 57004895100.

**Evgen Polyakov** – PhD Student of the Department of Airplanes and Helicopters Design, National Aerospace University "Kharkiv Aviation Institute", Kharkiv, Ukraine, e-mail: crpg\_emp@hotmail.com, ORCID: 0009-0002-6905-4595.